

Influence of dimensionality on thermoelectric device performance

Raseong Kim, Supriyo Datta, and Mark S. Lundstrom

Citation: *J. Appl. Phys.* **105**, 034506 (2009); doi: 10.1063/1.3074347

View online: <http://dx.doi.org/10.1063/1.3074347>

View Table of Contents: <http://jap.aip.org/resource/1/JAPIAU/v105/i3>

Published by the [American Institute of Physics](#).

Related Articles

Modeling and theoretical efficiency of a silicon nanowire based thermoelectric junction with area enhancement
J. Appl. Phys. **111**, 124319 (2012)

On the best bandstructure for thermoelectric performance: A Landauer perspective
J. Appl. Phys. **111**, 113707 (2012)

High-output-power densities from molecular beam epitaxy grown n- and p-type PbTeSe-based thermoelectrics via improved contact metallization
J. Appl. Phys. **111**, 104501 (2012)

Optimization of power and efficiency of thermoelectric devices with asymmetric thermal contacts
J. Appl. Phys. **111**, 024509 (2012)

Note: Extraction of temperature-dependent interfacial resistance of thermoelectric modules
Rev. Sci. Instrum. **82**, 116109 (2011)

Additional information on *J. Appl. Phys.*

Journal Homepage: <http://jap.aip.org/>

Journal Information: http://jap.aip.org/about/about_the_journal

Top downloads: http://jap.aip.org/features/most_downloaded

Information for Authors: <http://jap.aip.org/authors>

ADVERTISEMENT



AIP Advances

Now Indexed in
Thomson Reuters
Databases

Explore AIP's open access journal:

- Rapid publication
- Article-level metrics
- Post-publication rating and commenting

Influence of dimensionality on thermoelectric device performance

Raseong Kim,^{a)} Supriyo Datta, and Mark S. Lundstrom
 Network for Computational Nanotechnology, Discovery Park, Purdue University,
 West Lafayette, Indiana 47907, USA

(Received 5 December 2008; accepted 15 December 2008; published online 9 February 2009)

The role of dimensionality on the electronic performance of thermoelectric devices is clarified using the Landauer formalism, which shows that the thermoelectric coefficients are related to the transmission, $T(E)$, and how the conducting channels, $M(E)$, are distributed in energy. The Landauer formalism applies from the ballistic to diffusive limits and provides a clear way to compare performance in different dimensions. It also provides a physical interpretation of the “transport distribution,” a quantity that arises in the Boltzmann transport equation approach. Quantitative comparison of thermoelectric coefficients in one, two, and three dimensions shows that the channels are utilized more effectively in lower dimensions. To realize the advantage of lower dimensionality, however, the packing density must be very high, so the thicknesses of the quantum wells or wires must be small. The potential benefits of engineering $M(E)$ into a delta function are also investigated. When compared with a bulk semiconductor, we find the potential for $\sim 50\%$ improvement in performance. The shape of $M(E)$ improves as dimensionality decreases, but lower dimensionality itself does not guarantee better performance because it is controlled by both the shape and the magnitude of $M(E)$. The benefits of engineering the shape of $M(E)$ appear to be modest, but approaches to increase the magnitude of $M(E)$ could pay large dividends. © 2009 American Institute of Physics.

[DOI: 10.1063/1.3074347]

I. INTRODUCTION

The efficiency of thermoelectric devices is related to the figure of merit, $ZT = S^2GT/\kappa$,¹ where T is the temperature, S is the Seebeck coefficient, G is the electrical conductance, and κ is the thermal conductance, which is the sum of the electronic contribution κ_e and the lattice thermal conductance κ_l . The use of artificially structured materials such as superlattices² and nanowires^{3,4} has proven to be an effective way to increase the performance of thermoelectric devices by suppressing phonon transport. In addition to the success of phonon engineering, additional benefits might be possible by enhancing the electronic performance of thermoelectric devices.⁵ Possibilities include reducing device dimensionality^{6,7} and engineering the band structure.⁵

Using the Boltzmann transport equation (BTE),⁸ thermoelectric transport coefficients can be expressed in terms of the “transport distribution,” $\Xi(E)$.^{9,10} Note that the quantity $q^2\Xi(E)$ is sometimes called “differential conductivity,” $\sigma(E)$,^{11,12} where q is the electron charge. Mahan and Sofo⁹ showed mathematically that a delta-shaped $\Xi(E)$ gives the best thermoelectric efficiency. It has been also shown that the efficiency approaches the Carnot limit for a delta-shaped $\Xi(E)$ when the phonon heat conduction tends to zero.¹³

An alternative approach, the Landauer formalism,¹⁴ has been widely used in mesoscopic thermoelectric studies.^{15–18} In this paper, we show that it is also useful for macroscopic thermoelectrics. The Landauer formalism reduces to the diffusive results that can be also obtained from the BTE for large structures and to the ballistic results for small struc-

tures. It also provides a useful physical interpretation of conventional results from the BTE and a convenient way to compare performance across dimensions.

It has been reported that one-dimensional (1D) and two-dimensional (2D) structures may provide enhanced electronic performance due to the increased electrical conductivity per unit volume.^{6,7,19} Also, it has been argued that 1D thermoelectric devices will give better efficiencies because the density of states is close to a delta function.¹² Comparisons across dimensions, however, are not straightforward due to the issues such as the assumed cross section of nanowires and their packing density in a three-dimensional (3D) structure.²⁰

In this paper, our objective is to examine the role of dimensionality on the electronic performance of thermoelectric devices using the Landauer formalism. Similar comparisons have been done in the past,^{6,7} but comparisons across dimensions are often clouded by assumptions about the nanowire diameter and packing fraction. We present an approach that bypasses these issues. The paper is organized as follows. In Sec. II, we summarize the Landauer approach and present a physical interpretation of $\Xi(E)$, which turns out to be proportional to the transmission function, $\bar{T}(E)$.²¹ In Sec. III, we compare the Seebeck coefficient, S , and power factor (S^2G) in 1D, 2D, and 3D ballistic devices and discuss the role of dimensionality. In Sec. IV, scattering is briefly discussed and we examine the upper limit of performance possible by shaping $\bar{T}(E)$ into a delta function. Conclusions follow in Sec. V.

II. APPROACH

According to the Landauer formalism,¹⁴ the electrical current (I) and heat current are expressed as

^{a)}Electronic mail: kim369@purdue.edu.

$$I = \frac{2q}{h} \int T(E)M(E)(f_1 - f_2)dE \quad (\text{A}), \quad (1)$$

$$I_{q1} = \frac{2}{h} \int T(E)M(E)(E - E_{F1})(f_1 - f_2)dE \quad (\text{W}), \quad (2a)$$

$$I_{q2} = \frac{2}{h} \int T(E)M(E)(E - E_{F2})(f_1 - f_2)dE \quad (\text{W}), \quad (2b)$$

where I_{q1} and I_{q2} are the heating and cooling rates of contacts 1 and 2, respectively, and $I_{q2} - I_{q1} = \Delta VI$, where ΔV is the voltage difference between the contacts.²² In Eqs. (1) and (2), h is the Planck constant, $T(E)$ is the transmission, $M(E)$ is the number of conducting channels at energy E , E_{F1} and E_{F2} are the Fermi levels of the two contacts, and f_1 and f_2 are equilibrium Fermi–Dirac distributions for the contacts. In this paper, we assume a uniform conductor in which $T(E)$ is determined by scattering. Equations (1) and (2) apply to ballistic devices (commonly referred to as thermionic devices), as well as to diffusive devices (commonly referred to as thermoelectric devices). For ballistic devices, $T(E) = 1$, and for diffusive devices, $T(E) = \lambda(E)/(\lambda(E) + L) \approx \lambda(E)/L$, where $\lambda(E)$ is the energy-dependent mean free path and L is the length of the conductor.²³

In the linear response regime, $I_{q2} \approx I_{q1} \equiv I_q$, and Eqs. (1) and (2) are expressed as

$$I = G\Delta V + \overline{SG}\Delta T, \quad (3)$$

$$I_q = -\overline{TSG}\Delta V - \kappa_0\Delta T, \quad (4)$$

where ΔT is the temperature difference between contacts. Note that \overline{SG} is one quantity, not S times G . We set $E_F = E_{F1}$ and $f = f_1$, and the transport coefficients are

$$G = \frac{2q^2}{h} \int_{-\infty}^{\infty} \overline{T}(E) \left(-\frac{\partial f}{\partial E} \right) dE \quad (1/\Omega), \quad (5)$$

$$\overline{TSG} = -\frac{2q}{h} \int_{-\infty}^{\infty} \overline{T}(E)(E - E_F) \left(-\frac{\partial f}{\partial E} \right) dE \quad (\text{V}/\Omega), \quad (6)$$

$$\kappa_0 = \frac{2}{hT} \int_{-\infty}^{\infty} \overline{T}(E)(E - E_F)^2 \left(-\frac{\partial f}{\partial E} \right) dE \quad (\text{W}/\text{K}), \quad (7)$$

where $\overline{T}(E)$ is the transmission function,²¹ $\overline{T}(E) = T(E)M(E)$, and κ_0 is the electronic thermal conductance for zero electric field. Note that the units indicated in Eqs. (5)–(7) are the same in all three dimensions. Alternatively, Eqs. (3) and (4) can be expressed as

$$\Delta V = I/G - S\Delta T, \quad (8)$$

$$I_q = \Pi I - \kappa_e \Delta T, \quad (9)$$

where $S = \overline{SG}/G$, Π is the Peltier coefficient, $\Pi = -TS$, and $\kappa_e = \kappa_0 - TS^2G$.

Comparing the transport coefficients in Eqs. (5)–(7) with those from the BTE,⁹ we observe that the “transport distribution” $\Xi(E)$ (Refs. 9 and 10) has a simple, physical interpretation; it is proportional to $\overline{T}(E)$ as

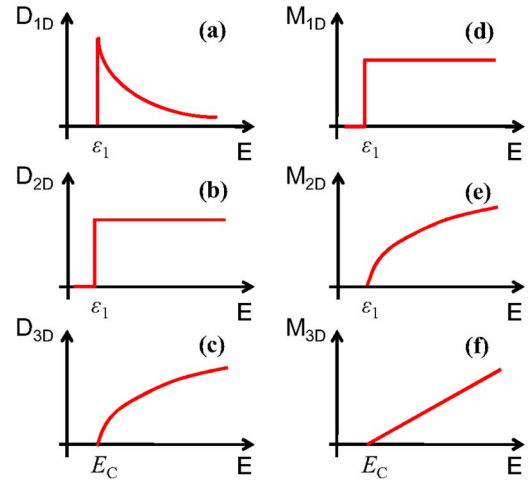


FIG. 1. (Color online) Sketches of [(a)–(c)] the density of states (D) and [(d)–(f)] the number of modes (M) for 1D, 2D, and 3D conductors with single parabolic subbands.

$$\Xi(E) = \frac{2}{h} \overline{T}(E) = \frac{2}{h} T(E)M(E), \quad (10)$$

where $M(E)$ essentially corresponds to the carrier velocity times the density of states,²¹ and $T(E)$ is a number between zero and one that is controlled by carrier scattering. [Note that $T(E)$ can also be engineered in quantum structures such as superlattices,^{24,25} a possibility not considered in this paper.]

In this section, we assume ballistic conductors with $T(E) = 1$. As noted earlier, the expressions for transport coefficients as given by Eqs. (5)–(7) are the same for all dimensions; only $M(E)$ changes. In this study, we will assume a simple energy band structure (although we believe that the overall conclusions are more general). If we assume that a single parabolic subband is occupied,

$$M_{1D}(E) = \Theta(E - \varepsilon_1), \quad (11a)$$

$$M_{2D}(E) = W \frac{\sqrt{2m^*(E - \varepsilon_1)}}{\pi\hbar}, \quad (11b)$$

$$M_{3D}(E) = A \frac{m^*}{2\pi\hbar^2} (E - E_C), \quad (11c)$$

where Θ is the unit step function, $\hbar = h/2\pi$, ε_1 is the bottom of the first subband, m^* is the electron effective mass, E_C is the conduction band edge, and W and A are the width and the area of the 2D and 3D conductors, respectively. Sketches in Fig. 1 clearly show the difference between the density of states and $M(E)$ for 1D, 2D, and 3D conductors. Using Eqs. (5)–(7) and (11a)–(11c), thermoelectric transport coefficients can be calculated and compared across dimensions as discussed in Sec. III.

III. RESULTS

In this section, we compare each component of ZT determined by electronic properties for 1D, 2D, and 3D ballis-

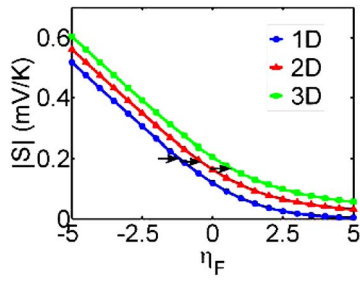


FIG. 2. (Color online) Model calculation ($T=300$ K) results for the $|S|$ vs η_F for 1D, 2D, and 3D ballistic conductors. For the same η_F , $|S_{3D}| > |S_{2D}| > |S_{1D}|$. The arrows indicate the magnitude of S at $\eta_{F,\max}$ where the power factor in Fig. 3 becomes the maximum in each dimension. We observe $|S_{1D}(\eta_{F,\max})| > |S_{2D}(\eta_{F,\max})| > |S_{3D}(\eta_{F,\max})|$.

tic conductors. Seebeck coefficients can be compared across dimensions directly because they have the same units in all dimensions. They are calculated from

$$S = \left(\frac{k_B}{-q} \right) \frac{\int M(E) [(E - E_F)/k_B T] \left(-\frac{\partial f}{\partial E} \right) dE}{\int M(E) \left(-\frac{\partial f}{\partial E} \right) dE} \quad (\text{V/K}), \quad (12)$$

where k_B is the Boltzmann constant. For the following model calculations, we assume $T=300$ K and $m^*=m_0$, where m_0 is the free electron mass. Figure 2 plots S versus η_F for 1D, 2D, and 3D ballistic conductors, where η_F is the position of E_F relative to the band edge, $\eta_F = (E_F - \varepsilon_1)/k_B T$. [To first order, S is independent of scattering as discussed in Sec. IV] Figure 2 shows that $|S_{3D}| > |S_{2D}| > |S_{1D}|$ for the same η_F . As shown in Eq. (12), S increases as the separation between E_F and $M(E)$ increases. As the dimensionality increases, $M(E)$ in Eq. (11) spreads out more, so S improves.

Although Fig. 2 shows that the magnitude of S is greater in 3D than in 1D or 2D for any η_F , there is more to the story. The power factor $S^2 G$ is an important part of the ZT . As shown in Fig. 3, the power factor displays a maximum at $\eta_{F,\max} = -1.14$, -0.367 , and 0.668 in 1D, 2D, and 3D, respectively. This occurs because the electrical conductance,

$$G = \frac{2q^2}{h} \int M(E) \left(-\frac{\partial f}{\partial E} \right) dE \equiv \frac{2q^2}{h} M_{\text{eff}} \quad (1/\Omega), \quad (13)$$

where M_{eff} is the effective number of conducting channels, increases more rapidly with η_F in 1D than in 2D or 3D as shown in Fig. 4. If we compare S not at the same η_F but rather at the $\eta_{F,\max}$ in each dimension, then $\hat{S} = |S(\eta_{F,\max})|$ is highest in 1D and lowest in 3D as indicated by the arrows in Fig. 2. For the specific case considered, $\hat{S}_{1D} = 2.29 \times k_B/q$, $\hat{S}_{2D} = 2.16 \times k_B/q$, and $\hat{S}_{3D} = 1.94 \times k_B/q$, which shows an 18% improvement in 1D over 3D.

The power factor is a key figure of merit for thermoelectric devices, but comparing power factors across dimensions brings up issues of the size and packing densities of the nanowires or quantum wells²⁰ because G is proportional to M_{eff} , which depends on W and A for 2D and 3D conductors, respectively. An alternative approach is to compare the

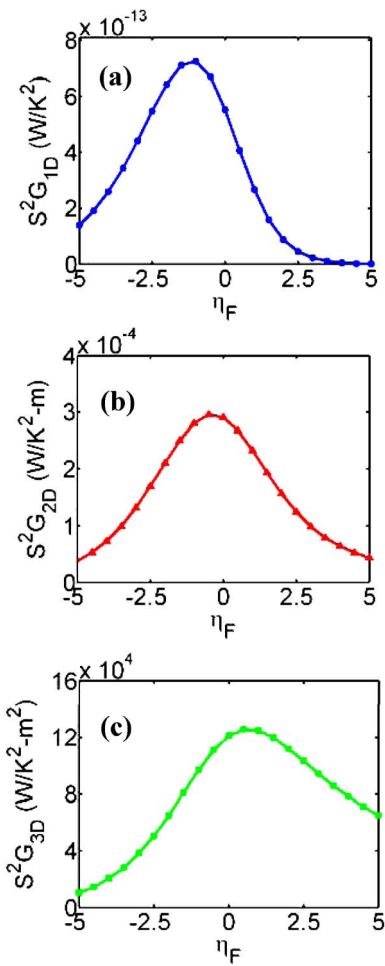


FIG. 3. (Color online) Model calculation ($m^*=m_0$, $T=300$ K) results for the power factor ($S^2 G$) vs η_F for (a) 1D, (b) 2D, and (c) 3D ballistic conductors. Power factor shows a maximum with $\eta_{F,\max} = -1.14$, -0.367 , and 0.668 in 1D, 2D, and 3D, respectively.

power factor per mode $S^2 G/M_{\text{eff}}$ at $\eta_{F,\max}$ for each dimensionality. The quantity $S^2 G/M_{\text{eff}}$ has the units (W/K^2) and can therefore be compared directly across dimensions. The results are $S^2 G/M_{\text{eff}}|_{1D} = 5.24 \times 2k_B^2/h$, $S^2 G/M_{\text{eff}}|_{2D} = 4.68 \times 2k_B^2/h$, and $S^2 G/M_{\text{eff}}|_{3D} = 3.75 \times 2k_B^2/h$. We observe that the modes are more effectively used in 1D and 2D than in 3D. In 1D, the power factor per mode is 40% larger than in 3D and 12% larger than in 2D. The benefits come from the fact that \hat{S} is highest in 1D and lowest in 3D.

So far, we have demonstrated that 1D thermoelectrics are superior to 3D thermoelectrics in terms of the Seebeck coefficient at the maximum power factor and in terms of the power factor per mode. To make use of 1D thermoelectric devices in macroscale applications, many nanowires must be placed in parallel, so issues of the nanowire size and packing density arise. To illustrate the considerations involved, we present a simple example. We first compute the maximum power factor for a 3D device ($S^2 G_{3D,\max}$) with an area of 1 cm^2 . For our model device with ballistic conduction, the result is $S^2 G_{3D,\max} = 12.6 \text{ W/K}^2$. We also find the number of effective conducting channels from Eq. (13) as $M_{\text{eff},3D} = 5.84 \times 10^{12}$. To compare this performance to a 2D thermoelectric device, we compute the maximum power factor of a

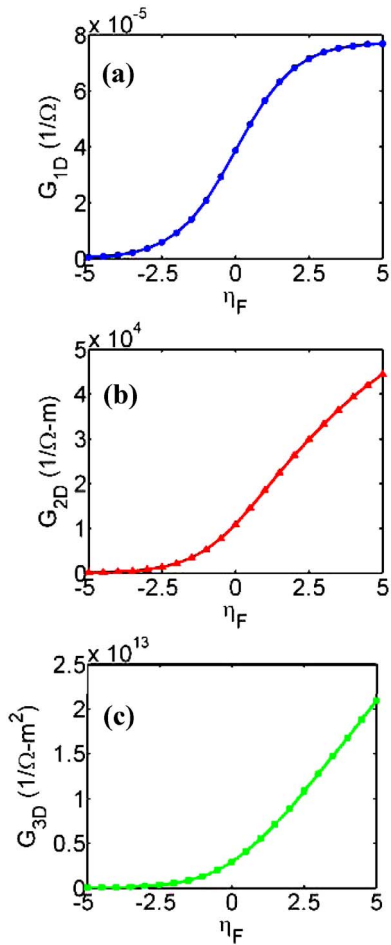


FIG. 4. (Color online) Model calculation ($m^*=m_0$, $T=300$ K) results for electrical conductance (G) vs η_F for (a) 1D, (b) 2D, and (c) 3D ballistic conductors. It increases more rapidly with η_F in 1D than in 2D or 3D.

2D device ($S^2G_{2D,\max}$) with $W=1$ cm, and the model calculation shows that $S^2G_{2D,\max}=2.96 \times 10^{-6}$ W/K² and $M_{\text{eff},2D}=1.10 \times 10^6$. Finally, we do the same for a 1D device and find $S^2G_{1D,\max}=7.28 \times 10^{-13}$ W/K² for $M_{\text{eff},1D}=0.242$.

The analysis presented earlier established that the power factor per mode is significantly better in 1D than in 2D, which is in turn better than 3D. To realize this advantage on the 1×1 cm² scale, we must produce the same number of effective modes in that area as is achieved in 3D. To do so (assuming 100% packing fraction), we find that the thickness of the 2D films must be less than $M_{\text{eff},2D}/M_{\text{eff},3D} \sim 1.89$ nm or the size of each nanowire must be less than $(M_{\text{eff},1D}/M_{\text{eff},3D})^{1/2} \times (M_{\text{eff},1D}/M_{\text{eff},3D})^{1/2} \sim 2.03 \times 2.03$ nm². Alternatively, we could seek to achieve the same power factor and ask what the size of the thin film or nanowire would need to be (still assuming a 100% packing fraction). The answer is 2D films with a thickness of $S^2G_{2D,\max}/S^2G_{3D,\max} \sim 2.35$ nm or 1D nanowires with a size of $(S^2G_{1D,\max}/S^2G_{3D,\max})^{1/2} \times (S^2G_{1D,\max}/S^2G_{3D,\max})^{1/2} \sim 2.40 \times 2.40$ nm². However we choose to look at it, the conclusion is that to realize the benefits of the inherently better thermoelectrics performance in 2D or 1D requires very small structures with very high packing fractions. In practice, nanowires or quantum wells should be separated by barriers,¹⁹ i.e., the “fill factor” should be less than 1. For

wires, the fill factor should be 1/4 to 1/3 to maintain their 1D properties.²⁰ This means that the advantages coming from the more nearly optimal distribution of modes for 1D systems are likely to be compensated by the limited fill factor, which reduces the total number of modes M_{eff} .

Finally, we should consider how different m^* might affect our conclusions. To first order, S is independent of m^* . In 1D, G is also independent of m^* because the m^* -dependencies in the density of states and the velocity cancel out.²⁶ In 2D $G_{2D} \propto \sqrt{m_{2D}^*}$, and in 3D $G_{3D} \propto m_{3D}^*$. Redoing the analysis presented above for $m^*=0.1m_0$, we find that the required sizes of the 2D films or 1D wires is about three times larger. Although the size and packing fraction requirements are still daunting, it appears that the use of low-dimensional structures may be more advantageous for low effective mass thermoelectric devices.

IV. DISCUSSION

Our analysis so far has assumed ballistic transport, $T(E)=1$; in the diffusive limit, $T(E) \rightarrow \lambda(E)/L$. For several common scattering mechanisms, $\lambda(E)$ can be expressed in power law form as $\lambda(E)=\lambda_0(E(p)/k_B T)^s$, where λ_0 is a constant, $E(p)$ is the kinetic energy, and s is the characteristic exponent, which depends on device dimensionality and the particular scattering mechanisms.²⁷ Using this form, the transport coefficients for diffusive thermoelectrics can be calculated from Eqs. (5)–(7). We compare the power factor per mode S^2G/M_{eff} for three cases: (i) an energy-independent $\lambda(E)$ with $s=0$, (ii) a constant scattering time (τ) with $s=1/2$, and (iii) scattering rates ($1/\tau$) proportional to the density of states, where s is 1, 1/2, and 0 for 1D, 2D, and 3D, respectively. In case (i), the results are the same as the ballistic case because S does not depend on scattering and G is simply scaled by a factor of λ_0/L . In case (ii), the modes are still utilized more effectively in lower dimensions as $S^2G/M_{\text{eff}}|_{1D}=4.68 \times 2k_B^2/h$, $S^2G/M_{\text{eff}}|_{2D}=3.75 \times 2k_B^2/h$, and $S^2G/M_{\text{eff}}|_{3D}=2.26 \times 2k_B^2/h$. In this case, the 40% improvement that we found in the ballistic case has become a 100% improvement of 1D over 3D. In case (iii), however, the power factor per mode is the same in all dimensions, $S^2G/M_{\text{eff}}=3.75 \times 2k_B^2/h$. A full treatment of the role of scattering is beyond the scope of this study. It involves more than the characteristic exponent because effects such as surface roughness scattering,^{28,29} enhanced phonon scattering,³⁰ and interaction with confined phonon modes³¹ may arise in 1D structures. From the solutions of the inelastic 3D Boltzmann equation, Broido and Reinecke³² have shown that there is a limit to the enhancement of the power factor in the quantum well and quantum wire because scattering rates increase with decreasing well and wire widths. The comparison of the electronic and lattice contributions to ZT for specific III–V nanowires considering all fundamental scattering mechanisms have shown that much of the ZT increase comes from the reduced κ_l .³³ Therefore, in the diffusive limit, we may or may not enjoy advantages in the electronic performance in lower dimensions depending on the details of the scattering processes. This issue deserves further study, but the broad conclusion obtained in Sec. III for ballistic conductors still

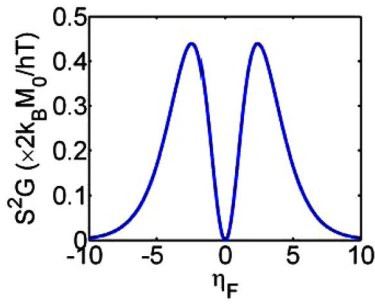


FIG. 5. (Color online) Calculation results for the power factor vs η_F for $M(E)=M_0\delta(E-E_C)$. The expression is shown in Eq. (14b). The maximum power factor appears at $\eta_F \sim \pm 2.4$ and the maximum value is $\sim 2k_B M_0 / h T \times 0.44$. At this maximum, the power factor per mode is $\sim 5.76 \times 2k_B^2 / h$

applies; the packing density of 1D and 2D devices must be high to exceed the absolute power factor of a 3D device, and the individual devices must be small.

Finally, we examine the upper limit performance possible by assuming that $M(E)$ has its ideal shape—a delta function. Mahan and Sofo⁹ showed that a delta-shaped $\Xi(E)$ gives the best thermoelectric efficiency because it makes the electronic heat conduction zero, $\kappa_e = \kappa_0 - TS^2G = 0$, which minimizes the denominator of ZT . For $M(E)=M_0\delta(E-E_C)$, we find

$$G_{\text{delta}} = \frac{2q^2}{h} M_0 \frac{1}{k_B T} \frac{e^{(E_C - E_F)/k_B T}}{(e^{(E_C - E_F)/k_B T} + 1)^2} \equiv \frac{2q^2}{h} M_{\text{eff}}, \quad (14a)$$

$$S^2 G_{\text{delta}} = \frac{2k_B^2}{h} M_0 \frac{1}{k_B T} \frac{e^{(E_C - E_F)/k_B T}}{(e^{(E_C - E_F)/k_B T} + 1)^2} \left(\frac{E_C - E_F}{k_B T} \right)^2. \quad (14b)$$

Figure 5 shows that $S^2 G_{\text{delta}}$ has two peaks at $\eta_F \sim \pm 2.4$ and that its maximum value $S^2 G_{\text{delta,max}} \sim 2k_B M_0 / h T \times 0.44$ is proportional to M_0 . At this maximum, the power factor per mode becomes $S^2 G / M_{\text{eff}}|_{\text{delta}} = 5.76 \times 2k_B^2 / h$. To explore the potential benefit from engineering $M(E)$, we compare the power factors calculated from $M_{3D}(E)$ in Eq. (11c) and $M_0\delta(E-E_C)$. We determine the M_0 that makes M_{eff} the same for the two cases for $A=1 \text{ cm}^2$ and then compare the maximum power factors. The result shows that $S^2 G_{3D,\text{max}} = 12.6 \text{ W/K}^2$ and $S^2 G_{\text{delta,max}} = 19.3 \text{ W/K}^2$. Therefore, shaping $M_{3D}(E)$ into a delta function gives a 53% improvement in power factor. It should be noted, however, that we have assumed that M_{eff} is the same in both cases. This is equivalent to comparing the power factor per mode, $(S^2 G M_{\text{eff}}|_{\text{delta}}) / (S^2 G M_{\text{eff}}|_{3D}) = 5.76 / 3.75 \sim 1.53$. We can also compare the $M_{2D}(E)$ in Eq. (11b) and $M_{1D}(E)$ in Eq. (11a) with the delta function. The comparison shows a 23% improvement over 2D and a 10% improvement over 1D power factors as $(S^2 G M_{\text{eff}}|_{\text{delta}}) / (S^2 G M_{\text{eff}}|_{2D}) = 5.76 / 4.68 \sim 1.23$ and $(S^2 G M_{\text{eff}}|_{\text{delta}}) / (S^2 G M_{\text{eff}}|_{1D}) = 5.76 / 5.24 \sim 1.1$. The advantage of the delta function decreases with decreasing dimensionality because the shape of $M(E)$ improves as dimensionality decreases.

As discussed above, the ideal delta-shaped $M(E)$ means that the power factor per mode is maximized and the modes are used most effectively. It should be noted, however, that

the magnitude of $M(E)$ is also important as well as the shape of it to increase the total power factor and ZT . Shaping $M(E)$ promises some benefit, but the benefits would also come by increasing $M(E)$. Therefore, it is worth exploring the possibilities of engineering both the shape and the magnitude of $M(E)$ to maximize the thermoelectric efficiency. Molecular thermoelectrics^{34,35} may have potential because $M(E)$ is inherently a broadened delta function, and its magnitude might be greatly increased by connecting many molecules in parallel. In another recent experiment,⁵ an increase in ZT was reported for bulk PbTe doped by Tl. This is believed to be due to the additional resonant energy level, which improves both the shape and magnitude of $M(E)$.

V. CONCLUSIONS

In this paper, we examined the role of dimensionality on the electronic performance of thermoelectric devices using the Landauer formalism. We showed that the transmission $T(E)$ and the number and distribution of conducting channels $M(E)$ are major factors determining thermoelectric transport coefficients. We also found that the “transport distribution”^{9,10} is proportional to the product $T(E)M(E)$. Assuming ballistic transport $T(E)=1$, we were able to show quantitatively how much more efficiently the modes are utilized in 1D than in 2D and 3D. It is hard, however, to realize the advantage because the quantum wires or wells should be closely packed, and their thicknesses should be very small. To first order, these conclusions also apply in the diffusive limit.

Using the Landauer approach, we also discussed the possible benefits from engineering $M(E)$ into a delta function. For the same effective number of conducting channels, the improvement over a parabolic band in 3D is about 50%. As dimensionality decreases, the shape of $M(E)$ becomes closer to a delta function. However, this does not necessarily mean that 1D is better than 2D or 3D because the magnitude of $M(E)$ is also important. It is not dimensionality itself that is important, it is the shape and the magnitude of $M(E)$. We conclude that reduced dimensionality per se, does not hold great promise for improving the electronic part of the figure of merit. Engineering band structures through size quantization, strain, crystal orientation, etc., should, however, be carefully explored in addition to the efforts to reduce κ_l .^{4,33}

ACKNOWLEDGMENTS

This work was supported by the National Science Foundation under Grant No. ECS-0609282. Computational support was provided by the Network for Computational Nanotechnology, supported by the National Science Foundation under Cooperative Agreement No. EEC-0634750. It is a pleasure to acknowledge helpful discussions with L. Siddiqui and A. N. M. Zainuddin at Purdue University, Professor Ali Shakouri at the University of California at Santa Cruz, and Dr. Rama Venkatasubramanian at the Research Triangle Institute.

¹H. J. Goldsmid, *Thermoelectric Refrigeration* (Plenum, New York, 1964).

²R. Venkatasubramanian, E. Siivola, T. Colpitts, and B. O’Quinn, *Nature*

- (London) **413**, 597 (2001).
- ³A. I. Boukai, Y. Bunimovich, J. Tahir-Kheli, J.-K. Yu, W. A. Goddard III, and J. R. Heath, *Nature (London)* **451**, 168 (2008).
- ⁴A. I. Hochbaum, R. Chen, R. D. Delgado, W. Liang, E. C. Garnett, M. Najarian, A. Majumdar, and P. Yang, *Nature (London)* **451**, 163 (2008).
- ⁵J. P. Heremans, V. Jovovic, E. S. Toberer, A. Saramat, K. Kurosaki, A. Charoenphakdee, S. Yamanaka, and G. J. Snyder, *Science* **321**, 554 (2008).
- ⁶L. D. Hicks and M. S. Dresselhaus, *Phys. Rev. B* **47**, 12727 (1993).
- ⁷L. D. Hicks and M. S. Dresselhaus, *Phys. Rev. B* **47**, 16631 (1993).
- ⁸N. W. Ashcroft and N. D. Mermin, *Solid State Physics* (Saunders College Publishing, Philadelphia, 1976).
- ⁹G. D. Mahan and J. O. Sofo, *Proc. Natl. Acad. Sci. U.S.A.* **93**, 7436 (1996).
- ¹⁰T. J. Scheidemantel, C. Ambrosch-Draxl, T. Thonhauser, J. V. Badding, and J. O. Sofo, *Phys. Rev. B* **68**, 125210 (2003).
- ¹¹A. Shakouri and C. LaBounty, in *Proceedings of the 18th International Conference on Thermoelectrics* (1999), pp. 35–39.
- ¹²G. Chen and A. Shakouri, *ASME J. Heat Transfer* **124**, 242 (2002).
- ¹³T. E. Humphrey and H. Linke, *Phys. Rev. Lett.* **94**, 096601 (2005).
- ¹⁴R. Landauer, *IBM J. Res. Dev.* **1**, 223 (1957).
- ¹⁵U. Sivan and Y. Imry, *Phys. Rev. B* **33**, 551 (1986).
- ¹⁶P. Streda, *J. Phys.: Condens. Matter* **1**, 1025 (1989).
- ¹⁷P. N. Butcher, *J. Phys.: Condens. Matter* **2**, 4869 (1990).
- ¹⁸H. v. Houten, L. W. Molenkamp, C. W. J. Beenakker, and C. T. Foxon, *Semicond. Sci. Technol.* **7**, B215 (1992).
- ¹⁹L. D. Hicks, T. C. Harman, X. Sun, and M. S. Dresselhaus, *Phys. Rev. B* **53**, R10493 (1996).
- ²⁰K. Chao and M. Larsson, *Physics of Zero- and One-Dimensional Nanoscopic Systems* (Springer, Berlin, 2007), Vol. 156, pp. 151–186.
- ²¹S. Datta, *Quantum Transport: Atom to Transistor* (Cambridge University Press, New York, 2005).
- ²²G. D. Mahan, *J. Appl. Phys.* **76**, 4362 (1994).
- ²³S. Datta, *Electronic Transport in Mesoscopic Systems* (Cambridge University Press, Cambridge, 1995).
- ²⁴L. W. Whitlow and T. Hirano, *J. Appl. Phys.* **78**, 5460 (1995).
- ²⁵A. Shakouri, *Proc. IEEE* **94**, 1613 (2006).
- ²⁶M. Lundstrom and J. Guo, *Nanoscale Transistors: Device Physics, Modeling and Simulation* (Springer, New York, 2006).
- ²⁷M. Lundstrom, *Fundamentals of Carrier Transport*, 2nd ed. (Cambridge University Press, Cambridge, 2000).
- ²⁸J. Wang, E. Polizzi, A. Ghosh, S. Datta, and M. Lundstrom, *Appl. Phys. Lett.* **87**, 043101 (2005).
- ²⁹S. Jin, M. V. Fischetti, and T.-W. Tang, *J. Appl. Phys.* **102**, 083715 (2007).
- ³⁰R. Kotlyar, B. Obradovic, P. Matagne, M. Stettler, and M. D. Giles, *Appl. Phys. Lett.* **84**, 5270 (2004).
- ³¹L. Donetti, F. Gamiz, J. B. Roldan, and A. Godoy, *J. Appl. Phys.* **100**, 013701 (2006).
- ³²D. A. Broido and T. L. Reinecke, *Phys. Rev. B* **64**, 045324 (2001).
- ³³N. Mingo, *Appl. Phys. Lett.* **84**, 2652 (2004).
- ³⁴M. Paulsson and S. Datta, *Phys. Rev. B* **67**, 241403 (2003).
- ³⁵P. Reddy, S.-Y. Jang, R. A. Segalman, and A. Majumdar, *Science* **315**, 1568 (2007).